

OPEN HEAVY FLAVOR PRODUCTION IN DEEPLY INELASTIC ep SCATTERING AT HERA*

KARIN DAUM†

Universität Wuppertal, Rechenzentrum, Gaußstraße 20

D-42097 Wuppertal, Germany

E-mail: daum@mail.desy.de

(On behalf of the H1 and ZEUS collaborations)

ABSTRACT

Recent results on inclusive D^0 and $D^{*\pm}$ production in deeply inelastic ep scattering at $\sqrt{s} = 301$ GeV are summarized. The data have been collected by the H1 and ZEUS experiments at HERA. The total and the differential cross sections are discussed in the framework of LO and NLO QCD predictions. The data exhibit clear evidence for boson gluon fusion dominating open heavy flavor production in the kinematic range currently explored at HERA. The measurements of $F_2^{c\bar{c}}(x, Q^2)$ at small Bjorken x are presented. The prospects for future analyses of open charm and beauty production including detector upgrades and anticipated high luminosities are investigated.

1. Introduction

The study of heavy flavor production in deeply inelastic lepton nucleon scattering (DIS) is of importance for the understanding of the parton densities in the nucleon^{1,2,3,4}. In accordance with early measurements by the EMC collaboration⁵, neutral current charm quark production is expected to be dominated by the *boson gluon fusion (BGF)* process $\gamma(Z^0)g \rightarrow c\bar{c}$ at large Bjorken x . Recent results on inclusive production of D^0 and $D^{*\pm}$ mesons from H1⁶ and ZEUS⁷ at HERA enable the charm production mechanism at small x to be investigated.

The measurement of the charm contribution $F_2^{c\bar{c}}(x, Q^2)$ to the proton structure function F_2 is supposed to provide information on this mechanism. Present parton density calculations include heavy flavors in the proton using different assumptions. Charm is either considered as *flavor excitation (FE)*, i.e. $\gamma(Z^0)q \rightarrow qX$, in the massless quark evolution starting with a charm density of zero at a scale Q_0^2 ^{8,9} or it is exclusively treated as BGF taking into account the charmed quark mass¹⁰. In terms of phenomenological inclusive analyses^{9,10,11} BGF is predicted to dominate near threshold, while FE should lead to a good description well above threshold. Various schemes to match these two regions have been proposed^{4,12}. Both approaches lead to similar predictions for $F_2^{c\bar{c}}(x, Q^2)$ but differences in exclusive heavy quark spectra are expected.

If charmed hadron production is dominated by BGF, it provides direct information

*To appear in Proc. of "New Trends in HERA Physics", Ringberg, May 1997

†presently at DESY, D-22603 Hamburg, Germany

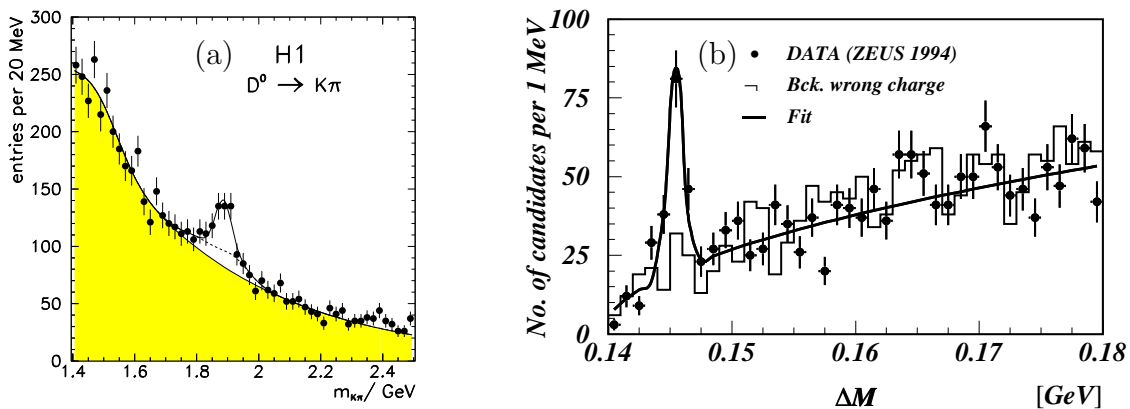


Fig. 1. (a) The $K^-\pi^+$ mass distribution observed in the D^0 analysis of DIS events from H1, and (b) the Δm distribution obtained in the D^{*+} analysis of DIS events from ZEUS.

on the gluonic content of the proton, $x_g g(x_g, Q^2)$, complementary to what is obtained from scaling violation analyses of F_2 . Since the reconstruction of hadrons with heavy flavor content unequivocally tags the parent quark, heavy quark spectra become directly accessible. Compared to two jet studies the analysis of charmed hadrons allows (a) to investigate the BGF process down to the phase space limit $\hat{s} = 4m_c^2$ which extends the range for the determination of the gluon density in the proton significantly towards smaller x_g , and (b) to tag the gluon in the proton almost free of background from FE of light quarks in the proton, since heavy flavor production from gluon splitting is suppressed by heavy quark masses.

2. Results

Published results on charm production in deeply inelastic ep scattering exist from both experiments H1 and ZEUS based on an integrated luminosity of roughly 3 pb^{-1} collected with each experiment at HERA in 1994. In addition preliminary results from ZEUS are available based on an integrated luminosity of 6.4 pb^{-1} from the HERA 1995 running. The H1 collaboration⁶ has performed the tagging of heavy quark events by reconstructing D^0 (1864)^a and D^{*+} (2010) mesons, while the ZEUS collaboration⁷ gives results for the inclusive D^{*+} (2010) analysis.

The D^0 is identified via its decay mode $D^0 \rightarrow K^-\pi^+$ and the D^{*+} through the decay chain $D^{*+} \rightarrow D^0\pi_{slow}^+ \rightarrow K^-\pi^+\pi_{slow}^+$. For the latter use is made of the low Q -value in the decay of $D^{*+} \rightarrow D^0\pi_{slow}^+$ which leads to a better resolution for the mass difference $\Delta m = m(D^0\pi_{slow}^+) - m(D^0)$ than for the D^{*+} mass itself.

Figure 1 shows the $m_{K\pi}$ distribution obtained in the inclusive D^0 analysis of H1 and the Δm distribution as observed in the inclusive D^{*+} of ZEUS. Evidently the number of observed events containing heavy quarks is small. Only of the order of 100 to 200 charmed mesons are identified in any of the different analyses.

^aCharge conjugate states are always included.

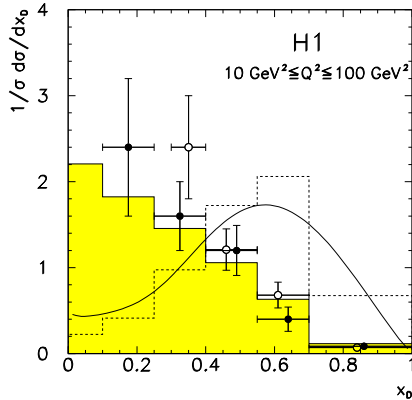


Fig. 2. Normalized x_D distribution in deep inelastic ep scattering at $\langle W \rangle \approx 125 \text{ GeV}$ for $|\eta_D| < 1.5$. The open/closed points represent the D^0/D^* data of H1. See text for further explanations.

2.1. Mechanism of charm production in DIS

Due to the hard fragmentation of D mesons its momentum is strongly correlated with the parent charm quark momentum. Therefore the distribution of the scaled D momentum in the γ^*p system $x_D = 2|\vec{P}_D^*|/W$ depends on the charm quark momentum spectrum and thereby on the mechanism of charm production. In BGF a $c\bar{c}$ pair is produced recoiling against the proton remnant in the γ^*p system, whilst in FE a single charmed quark is emitted opposite to the proton remnant, confining the second charmed quark necessary for quantum number conservation. Consequently the mean $\langle x_D \rangle$ of D mesons in the current and central fragmentation region is expected to be roughly a factor of 2 smaller for BGF compared to FE.

Figure 2 shows the distributions $1/\sigma \, d\sigma/dx_D$ obtained from the D^0 and D^{*+} analysis of H1 in comparison to the expectation for the BGF and FE process. The LO BGF prediction from AROMA¹³ (shaded histogram) agrees well with the data. The figure also includes the FE expectations for charmed mesons either by using the LEPTO 6.1 generator¹⁴, from which only FE events are selected (dashed histogram), or by extrapolating the results from charm production in charged current $(\bar{\nu})N$ scattering¹⁶ to HERA energies (full line). Large differences in the shape are observed for the data and these FE expectations. From a fit to the data of BGF and FE in arbitrary proportions it is concluded that more than 95% of neutral current charm production in DIS is due to the BGF process at $\langle Q^2 \rangle \approx 25 \text{ GeV}^2$. This observation seems to contradict recent inclusive calculations of charm production in DIS⁴, from which it was concluded that for the kinematic range of the current analyses at HERA charmed quarks may already be considered as massless partons in the proton.

2.2. Differential inclusive D^* cross sections

Figure 3 shows the differential $e^+p \rightarrow D^{*\pm}X$ cross sections as a function of a)

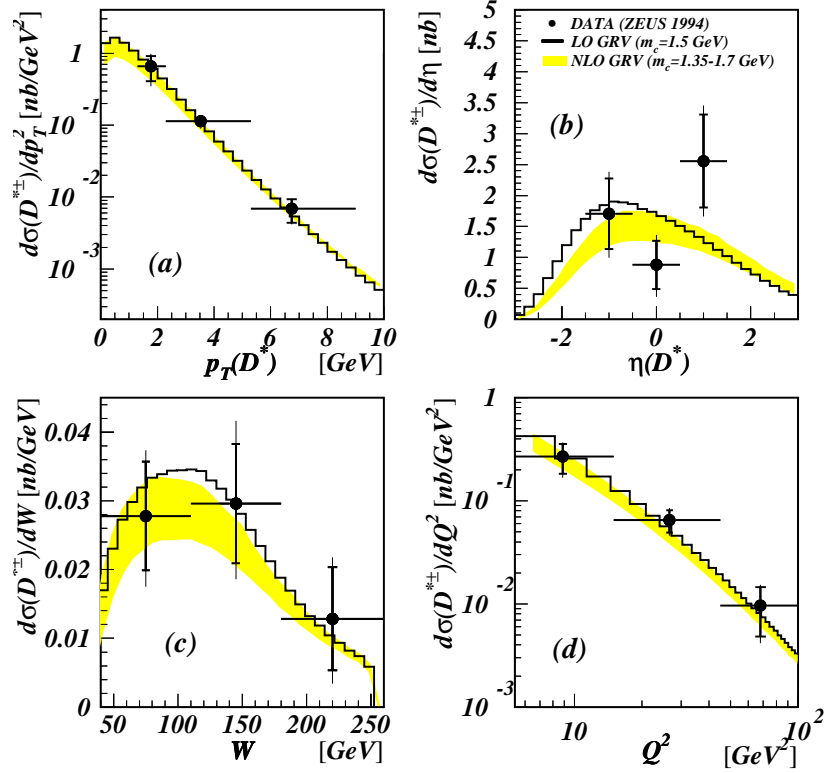


Fig. 3. Differential $e^+p \rightarrow D^{*\pm}X$ cross sections for $5 < Q^2 < 100 \text{ GeV}^2$, $y < 0.7$ in the kinematic region $1.3 < p_T(D^*) < 10 \text{ GeV}$, $|\eta(D^*)| < 1.5$ as a function of a) $p_T(D^*)$, b) $\eta(D^*)$, c) W and d) Q^2 from ZEUS. The inner/outer error bars correspond to the statistical/total errors respectively. The band and histogram are explained in the text.

$p_T(D^*)$, b) $\eta(D^*)$, c) W and d) Q^2 measured by ZEUS. The shaded band represents the result of the analytic NLO calculation³ using the GRV-HO 94¹⁰ gluon density of the proton which assumes charm being exclusively produced by BGF and treats charm quarks as massive particles. Both the renormalization scale and the factorization scale are set to $\mu = \sqrt{Q^2 + 4m_c^2}$. The largest uncertainties in the calculations arise from the ignorance of m_c . The upper (lower) limit corresponds to a charm quark mass $m_c = 1.35(1.7) \text{ GeV}$. This calculation reproduces well the shapes of the differential distributions. The figure also includes the analytic LO calculation as histograms. The LO calculation describes the shapes of the distributions equally well.

2.3. Integrated charm cross sections

All differential distributions discussed in the previous sections are found to be well described by the BGF process. Therefore, it is used to extrapolate the inclusive D cross sections, $\sigma(ep \rightarrow eDX)$, from the visible kinematic region to the full phase space in order to determine the charm production cross section, $\sigma(ep \rightarrow ec\bar{c}X)$, in DIS.

Table 1. Measured and predicted integrated charm cross sections $\sigma(ep \rightarrow ec\bar{c}X)$ for different bins in Q^2 in the region $y < 0.7$ (ZEUS) and $0.01 < y < 0.7$ (H1).

	m_c [GeV]	$5 < Q^2 < 10 \text{ GeV}^2$	$10 < Q^2 < 100 \text{ GeV}^2$
ZEUS $D^{*\pm}$		$13.5 \pm 5.2 \pm 1.8^{+1.6}_{-1.2}$ nb	$12.5 \pm 3.1 \pm 1.8^{+1.5}_{-1.1}$ nb
LO MC	1.5	12.5 nb	14.2 nb
LO GRV	1.5	11.0 nb	12.4 nb
NLO GRV	1.5	9.4 nb	11.1 nb
H1 $D^{*\pm}$			$15.1 \pm 1.8^{+2.4}_{-2.0} \pm 1.2$ nb
H1 D^0			$19.5 \pm 2.6^{+2.7}_{-2.5} {}^{+1.6}_{-1.2}$ nb
NLO MRSH	1.3		11.3 nb
NLO MRSH	1.7		8.1 nb
H1 F_2 fit	1.5		13.6 nb

Table 1 summarizes the experimental results together with the predictions of the NLO calculations ^{2,3} for different parton densities and different values of m_c . The extrapolation in phase space is calculated in NLO using the GRV-H0 gluon density in case of the ZEUS data while the acceptance for the H1 data is calculated using the MRSH gluon density. In both cases $m_c = 1.5 \text{ GeV}$ and $\mu = \sqrt{Q^2 + 4m_c^2}$ are chosen. The charm fragmentation is described by the Peterson function with $\epsilon_c = 0.035 \pm 0.009$ (ZEUS) and the symmetric Lund function with the standard setting of JETSET 7.4 (H1). The errors correspond to the statistical error, the experimental systematic uncertainty and the model dependent uncertainty respectively. The latter accounts for the possible variation of the relevant parameters of the model used for extrapolation, i.e. $xg(x, Q^2)$, m_c , μ and the fragmentation function. In the region of overlap the cross section inferred from the $D^{*\pm}$ analyses are in reasonable agreement. The cross section from the D^0 analysis is higher but the few statistics do not allow any conclusion to be drawn.

In table 1 the data is also compared with predictions from analytic NLO calculations for different gluon densities and different values of m_c . Also given are LO analytic calculations and the result from the LO Monte Carlo. In addition H1 has performed a NLO calculation using the gluon density as derived from the analysis of scaling violations of F_2 ¹⁷. Within reasonable variations of the most relevant parameter, m_c , the NLO calculations tend to be below the experimental results except for the gluon density obtained from the NLO F_2 fit. The LO analytic calculation and the LO MC yield cross sections generally in better agreement with the data.

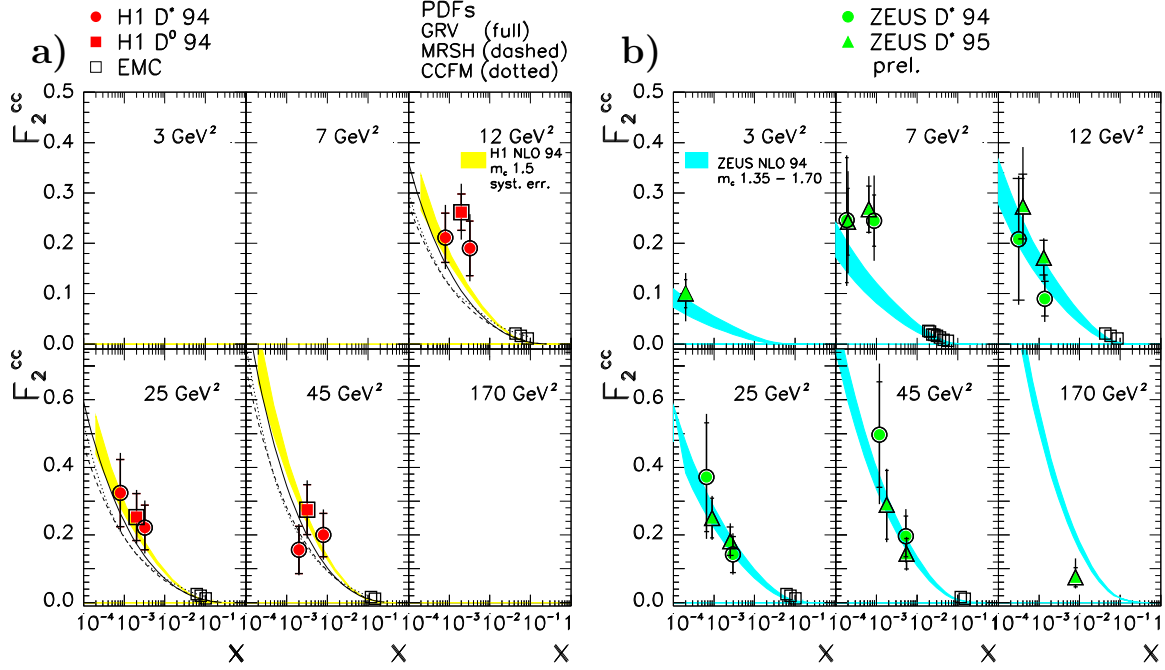


Fig. 4. The charm contribution $F_2^{c\bar{c}}$ to the proton structure function as derived (a) from the D^{*+} (dots) and D^0 analysis (squares) by the H1 collaboration and (b) from the D^{*+} by the ZEUS collaboration from the 1994 data (dots) and the 1995 data (triangles). The inner/outer error bars refer to the statistical/total errors. The EMC data are also shown (open boxes). The shaded band represent the predictions from the NLO fits to the H1 and ZEUS F_2 measurements respectively. The ZEUS 1995 data and the prediction of the NLO fit to the F_2 measurement are preliminary. In (a) predictions from NLO calculations based on GRV-HO (full line), MRSH (dashed line) and CCFM (dotted line) gluon densities using a charmed quark mass of $m_c = 1.5$ GeV are included

2.4. Charm contribution $F_2^{c\bar{c}}$ to the proton structure

The charm contribution $F_2^{c\bar{c}}$ to the structure function is obtained by using the expression for the one photon exchange cross section for charm production

$$\frac{d^2\sigma^{c\bar{c}}}{dx dQ^2} = \frac{2\pi\alpha^2}{Q^4 x} [1 + (1-y)^2] F_2^{c\bar{c}}(x, Q^2). \quad (1)$$

The contribution from Z exchange is expected to be small in the kinematic range explored presently. The $F_L^{c\bar{c}}$ contribution has been estimated to be negligible^{18,19}. Therefore both $F_3^{c\bar{c}}$ and $F_L^{c\bar{c}}$ are neglected.

The $F_2^{c\bar{c}}$ measurements from H1 and ZEUS are displayed in figure 4 together with the results from the EMC collaboration at large x . Within the limited statistics the results on $F_2^{c\bar{c}}$ from H1 and ZEUS are in good agreement. The measurements at HERA extend the range of the $F_2^{c\bar{c}}$ measurements by two orders of magnitude towards smaller x values. The comparison of the HERA and EMC data reveals a step rise of $F_2^{c\bar{c}}$ with decreasing x . H1 has derived a ratio of $F_2^{c\bar{c}}/F_2$ of

$$\langle F_2^{c\bar{c}}/F_2 \rangle = 0.237 \pm 0.021 \pm 0.041, \quad (2)$$

which is an increase of about one order of magnitude of the overall charm contribution compared to the EMC result. This is consistent with the measured rise of the gluon distribution towards low x and the dominance of the BGF process observed here. Within the accuracy of the charm data this ratio seems to be constant in the kinematic range explored in the H1 analysis.

The data are also compared to the NLO calculations of $F_2^{c\bar{c}}$ based on the gluon densities extracted from the NLO fits to the inclusive F_2 . In figure 4a the prediction from the H1 F_2 data, using a charmed quark mass of $m_c = 1.5$ GeV, is shown by an error band which includes the propagation of the statistical and the uncorrelated systematic errors on the total F_2 data through the fitting procedure. The uncertainty in the prediction of $F_2^{c\bar{c}}$ due to variations of m_c is indicated by the error band in figure 4b for the ZEUS F_2 data. The upper and lower limits correspond to $m_c = 1.35$ GeV and $m_c = 1.7$ GeV respectively. No error propagation in the fit is performed. In the region of overlap in Q^2 the H1 result of this fit favors a slightly larger gluon density at small x compared to the ZEUS measurement.

Figure 4a also includes the predictions from the NLO calculation based on GRV-HO, MRSH and CCFM²⁰ gluon density calculations. Although the procedures for treating heavy flavors and for determination of the gluonic content in the proton are quite different for these three parton density calculations, the resulting predictions for $F_2^{c\bar{c}}$ are very similar. The accuracy of the data in terms of statistical and systematic uncertainty is by far not sufficient to be able to get more insight on the gluon in the proton from purely inclusive charm measurements.

3. Future

Although the charm production cross section is found to be about 25% of the total DIS cross section at HERA, the number of identified charm events is fairly small at present. For the results presented here heavy flavor tagging is performed by the reconstruction of charmed hadrons. From the experimental point of view one advantage of this method is the small contribution to the systematic uncertainties due to hadronization effects. Furthermore, as a consequence of the hard fragmentation of charm quarks, the reconstructed charmed hadron gives direct access to the parent charm quark. This allows the study of the production dynamic of heavy quarks almost free of background from other processes. The drawback of this tagging method is the small tagging efficiency ($\epsilon_{tag} \approx \mathcal{O}(10^{-3})$) due to the small probability that a heavy quark fragments into a specific heavy flavored hadron which subsequently decays into the desired decay mode, e.g. for the chain $c \rightarrow D^{*\pm} X \rightarrow D^0 \pi_s^\pm X \rightarrow (K^\mp \pi^\pm) \pi_s^\pm X$ this probability is only $6.7 \cdot 10^{-3}$.

In order to increase ϵ_{tag} of heavy flavor production a Silicon Vertex Detector is installed in H1 this year (1997) and will be installed in ZEUS together with the luminosity upgrade of the HERA machine in 1999/2000. Such a device enables

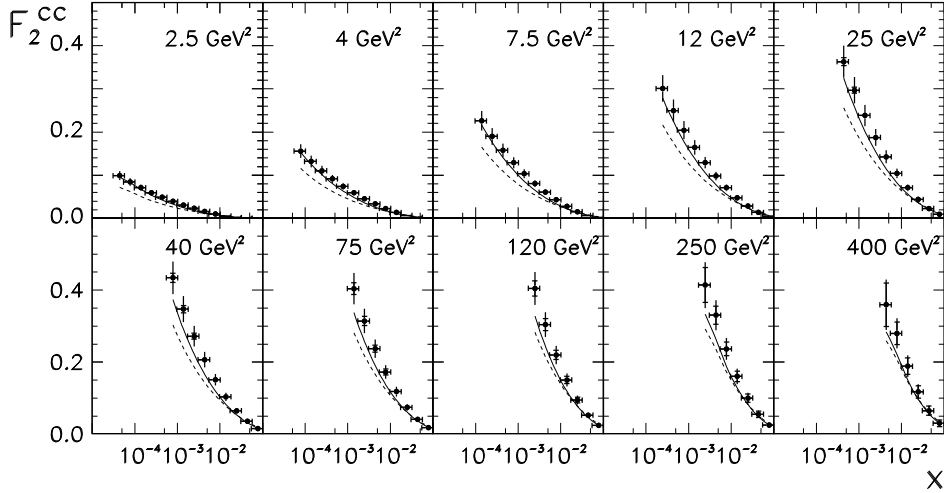


Fig. 5. The charm contribution $F_2^{c\bar{c}}$ as expected for an integrated luminosity of $\mathcal{L}_{int} \approx 200 \text{ pb}^{-1}$ using fully reconstructed charmed hadrons together with the Silicon Vertex Detector.

the reconstruction of the decay vertices of heavy flavored hadrons and will thereby suppress the combinatorial background in the mass reconstruction of heavy flavored hadrons. The reduction of background will give access to a large variety of decay modes with good signal to background ratios. Considering the analysis of all accessible decay modes together ϵ_{tag} will be increased by about one order of magnitude.

Alternatively heavy flavor events may be tagged by secondary vertices (SVTX) having high significance without explicit reconstruction of heavy flavored hadrons. This method will lead to tagging efficiencies comparable or even superior to the efficiency expected from the mass reconstruction method. Due to the absence of a mass constraint the SVTX method is expected to have larger background from faked secondary vertices. A much better understanding of fragmentation, detector and reconstruction performance is needed in this case to achieve experimental systematic uncertainties comparable to those of the mass reconstruction method. Furthermore it will become more difficult to access exclusive quantities of the production dynamics since the strong correlation between the heavy flavored hadron and the parent quark gets lost or will be weakened in partly reconstructed heavy flavored hadrons.

Figure 5 shows the expected accuracy of $F_2^{c\bar{c}}$ measurements for an integrated luminosity of $\mathcal{L}_{int} \approx 200 \text{ pb}^{-1}$ using fully reconstructed charmed hadrons together with the Silicon Vertex Detector. The data points show the expectation based on the gluon density extracted from the H1 NLO fit to the total F_2 for $m_c = 1.5 \text{ GeV}$ and $\mu^2 = Q^2 + 4m_c^2$. The inner/outer error bars refer to the statistical/total errors. Also shown are the NLO predictions for the GRV-HO (full line) and MRSH (dashed line) parton densities and the same charm mass and scales. At low Q^2 the measurement will be limited by the experimental uncertainty while at large Q^2 the precision will be limited by statistics. The ultimate precision of 10 % will allow these parameterizations of the gluon density to be distinguished.

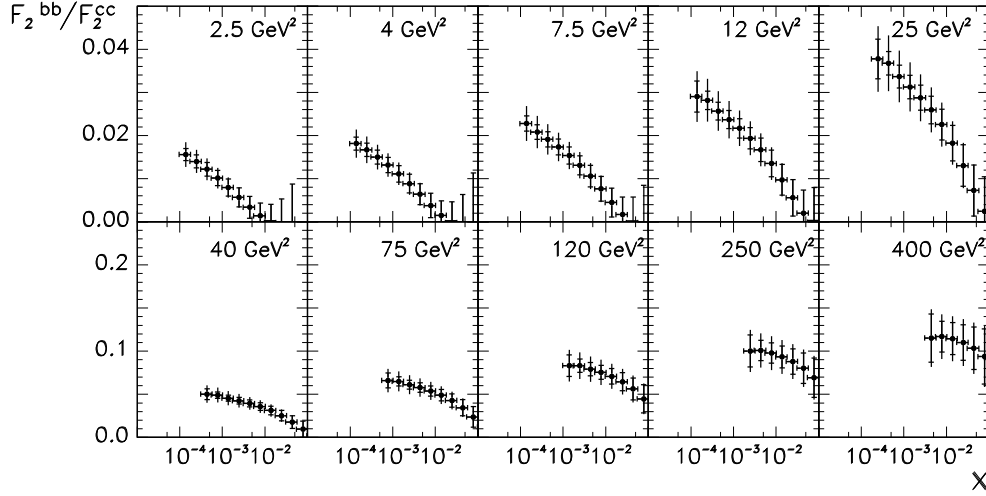


Fig. 6. The ratio F_2^{bb}/F_2^{cc} as expected for an integrated luminosity of $\mathcal{L}_{int} \approx 500 \text{ pb}^{-1}$ using fully reconstructed charmed hadrons together with the Silicon Vertex Detector.

Figure 6 shows the expected accuracy of the ratio F_2^{bb}/F_2^{cc} for an integrated luminosity of $\mathcal{L}_{int} \approx 500 \text{ pb}^{-1}$ using fully reconstructed charmed hadrons together with the Silicon Vertex Detector ¹⁹. Even for a luminosity of $\mathcal{L}_{int} \approx 500 \text{ pb}^{-1}$ the measurement of this ratio will be limited by statistics in the full x and Q^2 plane. For a given Q^2 or x the ratio is expected to rise with decreasing x or increasing Q^2 , respectively. A mean value of $\langle F_2^{bb}/F_2^{cc} \rangle \approx 0.02$ is predicted.

4. Conclusions

First results on charm production in deeply inelastic ep scattering at HERA have been presented. The investigation of differential D cross sections has shown that the production dynamics of charmed mesons in the current and central fragmentation region may be described by the boson gluon fusion process. The contribution from flavor excitation of charm in this region is found to be negligible at $\langle Q^2 \rangle \approx 25 \text{ GeV}^2$. This observation sets constraints on the kinematic region where charm may be treated as massless parton in the proton.

The measurement of $F_2^{cc}(x, Q^2)$ at small x reveals a strong rise of $F_2^{cc}(x, Q^2)$ from the fixed target to the HERA regime. Agreement is observed between the measured F_2^{cc} and the results from the NLO fits to the inclusive F_2 . Averaged over the kinematic range currently explored a ratio $\langle F_2^{cc}/F_2 \rangle = 0.237$ is observed which is one order of magnitude larger than at large x .

An estimation on the accuracy for the exploration of charm and beauty contribution F_2^{cc} and F_2^{bb} to the structure of the proton for an integrated luminosity of more than 200 pb^{-1} has been summarized. For $Q^2 \leq 100 \text{ GeV}^2$ the charm analysis will be systematically limited. The heavy flavor data will allow a direct measurement of the gluon density in the proton to be performed. A precision on $xg(x, Q^2)$ of 10 % may

be achieved from charm data, which is competitive with other methods. Despite of the smallness of the ratio $F_2^{b\bar{b}}/F_2^{c\bar{c}}$ high luminosity running will allow detailed studies of beauty production dynamics.

5. References

1. A. Ali *et al.*, in *Proc. of the HERA Workshop*, Hamburg, Vol. 1, 393 (1988), A. Ali and D. Wyler, in *Proc. of the Workshop "Physics at HERA"*, Hamburg, Vol. 2, 667 (1991) (and references therein).
2. E. Laenen *et al.*, *Nucl. Phys.* **B392** 162, 229, S. Riemersma *et al.*, *Phys. Lett.* **B347** (1996) 143.
3. B.W. Harris and J. Smith, *Nucl. Phys.* **B452** (1995) 109, FSU-HEP-970527, [hep-ph/9706334].
4. M.A.G. Aivazis *et al.*, *Phys. Rev.* **D50** (1994) 3085, 3102.
5. EMC Coll., J.J. Aubert *et al.*, *Nucl. Phys.* **B231** (1983) 31.
6. H1 Coll. C. Adloff *et al.*, *Z. Phys.* **C72** (1996) 539.
7. ZEUS Coll. J. Breitweg *et al.*, *DESY preprint*, *DESY 97-089*.
8. A.D. Martin, R.G. Roberts, and W.J. Stirling: *Phys. Lett.* **B306** (1993), 145, *Phys. Rev.* **D50** (1994) 6743, *Phys. Rev.* **D50** (1994) 6734.
9. A.D. Martin, *this proceedings* (and references therein).
10. M. Glück, E. Reya, and A. Vogt: *Z. Phys.* **C 53** (1992) 127, *M. Z. Phys.* **C 67** (1995) 433, A. Vogt, *this proceedings* (and references therein).
11. J. Smith, *this proceedings* (and references therein).
12. A.D. Martin *et al.*, DPT-96-102 and hep-ph/9612449, M. Buza *et al.*, DESY 96-258 and hep-ph/9612398.
13. G. Ingelman, J. Rathsman, and G.A. Schuler: *DESY preprint*, DESY 96-058, and hep-ph/9605285.
14. G. Ingelman: "*LEPTO version 6.1 - The Lund Monte Carlo for Deep Inelastic Lepton-Nucleon Scattering*", TSL/ISV-92-0065.
15. T. Sjöstrand: "*PYTHIA 5.7 and JETSET 7.4 Physics and Manual*", CERN-TH.7112/93.
16. H. Abramowicz *et al.*, CDHS Coll.: *Z. Phys.* **C15** (1982) 19, N. Ushida *et al.*, E531 Coll.: *Phys. Lett.* **B206** (1988) 380.
17. S. Aid *et al.*, H1 Coll.: *Nucl. Phys.* **B470** (1996) 3.
18. E. Leanen *et al.*, *Nucl. Phys.* **B392** (1993) 162, S. Riemersma *et al.*, *Proc. of the Workshop "Future Physics at HERA"*, DESY, Hamburg Vol. 1 (1995/96) 393.
19. K. Daum *et al.*, *Proc. of the Workshop "Future Physics at HERA"*, DESY, Hamburg Vol. 1 (1995/96) 89.
20. J. Kwieciński, A.D. Martin and P.L. Sutton, *Phys. Rev.* **D53** (1996) 6094, *Z. Phys.* **C71** (1996) 585, G.P. Salam, *this proceedings* (and references therein).